

# NUCLEAR ANALYSIS OF BULK SHIELDING FUSION INTEGRAL EXPERIMENTS ON LARGE SS316/WATER ASSEMBLY WITH SIMULATED SUPER CONDUCTING MAGNET

Mahmoud Z. Youssef\*, Anil Kumar\*, Mohamed A. Abdou\*, Chikara Konno+, Fujio Maekawa+, and Yujiro Ikeda+

\* School of Engineering and Applied Science,  
University of California at Los Angeles  
Los Angeles, CA, 90095, USA  
(310) 825-2879

+ Department of Reactor Engineering,  
Japan Atomic Energy Research Institute,  
Tokai-mura, Ibaraki-ken 319-11, Japan

## ABSTRACT

As part of a collaboration with Japan, the U.S. participated in several fusion integral experiments that simulate the design features of the shielding blanket of the International Thermonuclear Experimental Reactor, ITER. The purpose of these efforts is to resolve the critical issues associated with the neutronics R&D tasks of ITER, among which is the adequacy of the newly developed FENDL-1 database. For that purpose, JAERI has constructed a cylindrical test assembly of dimension 1.2 D x 1.2 L m and made of front multi-layers of SS316 and water with an embedded smaller zone consists of multi-layers of super conducting magnet (SCM) stimulant and SS316. Measured parameters, covering the neutron energy range from 14 MeV down to thermal energy, were taken inside the SS316 and the SCM layers at 9 locations up to a depth of 91.4 cm. In one experiment (Assembly#1), a 1.27 cm B<sub>4</sub>C + 3.8 cm Pb layer was added in front of the SCM multi-layer zone. This layer is not included in Assembly#2. As in previous experiments, the 14 MeV source is housed inside a source reflector can (20 cm-thick) and located at a distance of 30 cm from the assembly. The U.S. analysis reported here was performed with 175n-42g FENDL/MG-1.0 (multigroup) as well as ENDF/B-VI data using the DORT 2-D code. Analysis was also performed with the Monte Carlo (MC) continuous energy data, FENDL/MC-1.0. The calculated parameters were compared to the following measured data: (a) neutron spectrum below 2 MeV, (b) foil activation rates such as Nb-93(n,2n)Nb-93m, Al-27(n,α)Na-24, In-115(n,n')In-115m, Au-197(n,γ)Au-198, and B-10(n,α)Li-7, (c) fission rate U-235(n,f) and U-238(n,f), (d) gamma-ray spectrum, and (e) gamma-ray heating rate.

## 1. INTRODUCTION

The Engineering Design Activity (EDA) phase of ITER<sup>(1,3)</sup> is currently near completion. During this phase, several R&D activities in the area of nuclear design have been undertaken to ensure a sound nuclear performance of

the blanket and shield components. To verify the prediction capability of the current design codes and data bases in accessing the key nuclear parameters (e.g. nuclear heating, damage to super conducting magnet, etc), several integral experiments have been performed on assemblies that closely simulate ITER blanket/shield design. Pure SS316 assemblies were constructed<sup>(4-7)</sup> to represent those isolated components that do not require cooling. In addition, the data gained from performing experiments on these pure SS316 were used as a reference point to the data extracted from performing similar measurements and analyses on assemblies with different combination of structural material (SS316) and coolant (water). In the later series of experiments, multi-layers of SS316 and water were introduced in the assembly to simulate ITER cooled blanket<sup>(8-10)</sup>. To simulate the blanket/shield component which protects the magnet (and personnel) from nuclear field, a zone which simulates the super conducting magnet (SCM) was introduced in the SS316/water assemblies. Measurements were compared to analytical results to arrive at estimate of the accuracy in calculating the relevant nuclear parameters under these experimental conditions.

Among the issues examined is the accuracy of the present nuclear data base. The Nuclear data Section (NDS) of the International Atomic Energy Agency (IAEA) has provided the fusion community with newly developed nuclear data bases for fusion application in two versions, namely, the Fusion Nuclear Data Library FENDL-1<sup>(11-12)</sup> and FENDL-2<sup>(13-14)</sup>. FENDL-1 is undergoing an extensive benchmarking against existing differential and integral fusion neutronics experiments<sup>(8-16)</sup> in order to provide high quality assurance data base for ITER designers. Effort has already started to generate FENDL-2.0<sup>(13-14)</sup> which will also require detailed benchmarking.

The experiments performed so far within the U.S./Japan collaboration are: (1) bulk shielding experiment on a 1.2 m by 1.1176 m cylindrical assembly of SS316 without a source can, (2) bulk shielding experiment on a 1.2 m by 1.1176 m cylindrical assembly of SS316 with a source can (source reflector of 0.2 m thickness), (3) bulk shielding experiment on a 1.2 m by

1.3716 m cylindrical assembly of SS316/water multilayers with a source can, (4) bulk shielding experiment on a 1.2 m by 1.3716 m cylindrical assembly of SS316/water multilayers with a source can and with a simulated Super Conducting Magnet (SCM) zone, and (5) streaming experiments through Gaps.

The present work focuses on the experiment #4 above. The experiments and the associated analyses conducted on the SS316 assembly (#1 and #2 above) have been reported previously with FENDL multigroup data<sup>(6)</sup> (FENDL/MG-1.0) as well as FENDL Monte Carlo (FENDL/MC-1.0) data performed by JAERI<sup>(7)</sup>. JAERI has also performed the analysis on the SS316 assemblies<sup>(4-5)</sup> (#1 and #2) with JENDL-3.1 data base<sup>(18)</sup>. Results based on benchmarking both the multigroup library and the Monte Carlo library of FENDL using the SS316/water assembly can be found in Reference 10. The JAERI's parallel analysis based on JENDL-3.1 data can be found in References 8 and 9.

The analysis of the U.S. based on FENDL-1/multigroup and FENDL-1/MC data bases is given here for experiment #4 above. Results based on ENDF/B-VI data are also given for comparison. It was necessary to generate data libraries that include self-shielding correction for SS316 cross-sections when using multigroup data form. This is not necessary when using the MC form of FENDL since this data is continuous in energy. Section II describes the experiments analyzed and the measured items. Description of the procedures followed in the analysis is given in Section III. Results of FENDL/MG-1.0 and ENDF/B-VI benchmarking are given in Section IV. Section V is devoted to the observed discrepancies between the analytical results and measured data.

## II EXPERIMENTAL SET-UP AND MEASURED DATA

The cylindrical assembly is 120 cm in diameter and consists of alternating layers of SS316 and water up to a depth of 60.9 cm followed by 1.27 cm B<sub>4</sub>C + 3.8 cm Pb. Epoxy glass layer (2.54 cm) followed. The rest of the assembly is made of alternating layers of SCM material and SS316. A 2.54 cm-thick layer of epoxy glass (EG) is added at the back. Total assembly depth is 121.9 cm. The assembly has a source reflector can (20 cm-thick) as in previous experiments to lessen room return effect and simulate low-energy reflected source neutron component. Figure 1 depicts the assembly dimensions and composition. The atomic density of the materials used can be found in Table I.

Two assemblies were considered, namely: Assembly#1: The B<sub>4</sub>C/Pb layer is included, Assembly#2:

The B<sub>4</sub>C/Pb layer is replaced by SS316. Measured parameters, covering the neutron energy range from 14 MeV down to thermal energy, were taken inside the SS316 and the SCM layers at 9 locations (8 in Assembly#1) up to a depth of 91.4 cm. Calculated parameters were compared to the following measured items: (1) neutron spectrum in the range  $2 \text{ MeV} < E_n$ , measured by  $^{149}\text{Sm}$  (measurements made but not used), in the range  $3 \text{ keV} < E_n < 1 \text{ MeV}$  measured by Proton Recoil Counter (PRC) and in the range  $E_n < 10 \text{ keV}$  measured by BF<sub>3</sub> Counters, (2) foil activation rate of the reactions  $^{93}\text{Nb}(n,2n)^{92m}\text{Nb}$ ,  $^{27}\text{Al}(n,\alpha)^{24}\text{Na}$ ,  $^{115}\text{In}(n,n')^{115m}\text{In}$ ,  $^{197}\text{Au}(n,\gamma)^{198}\text{Au}$ ,  $^{10}\text{B}(n,\alpha)^7\text{Li}$ , (3) fission rate  $^{235}\text{U}(n,f)$ , (4) gamma-ray spectrum, and (5) gamma-ray heating rate measured by TLD. The dosimetry cross-sections for  $^{115}\text{In}(n,n')^{115m}\text{In}$  and  $^{235}\text{U}(n,f)$  reactions are taken from dosimetry data of JENDL-3.1<sup>(18)</sup>. The cross-sections for other reactions are from FENDL/MG-1.0 (based on ENDF/B-VI data).

The Calculated-to-the Experimental (C/E) values for the integrated neutron spectrum in the above mentioned energy ranges are given in the present work in addition to the C/E values for the other items listed above.

## III CALCULATION PROCEDURES

The 175n-42g FENDL/MG-1.0 in MATXS format was used in the benchmarking. The shielded and unshielded multigroup data libraries were generated in group-independent (GIP) form using the TRANSX2 processing code package<sup>(19,20)</sup>. Self shielding was considered an important correction since the total macroscopic cross-section of SS316 has many resonances in the energy range keV to few MeV. Neutrons lose energies through either elastic (many collisions) or inelastic collisions and ignoring the presence of these resonances will give an inaccurate flux estimates in SS316, particularly at deep locations and for low-energy neutrons.

JAERI has provided UCLA with the angular/energy distribution of the emitted neutrons from the tritiated-titanium target in 125 neutron group structure and 37 angles spanning (in 3-degree intervals) the directions from  $\mu=-1$  (180-degree) to  $\mu=+1$  (0-degree) along the z-axis. The incident neutron source was calculated by JAERI using the Monte Carlo code MORSE-DD<sup>(17)</sup>. The slowing down of deuteron ions in the TiT target, the shape of the deuteron beam, the kinematics of the D-T reactions, the cross-section of the D-T reaction at each deuteron energy, and the accurate description of the structural shape of the TiT target were taken into consideration. The peak energy of the source in the forward direction is at 14.8 MeV whereas it is 13.3 MeV in the backward direction. The

source has non-negligible low-energy component resulting from the interaction of the D-T neutrons with the structural material of the TiT target.

In the multigroup analysis, the RUFF code<sup>(21)</sup> was used to generate the uncollided flux and first collision source as input for the 2-D discrete ordinates code, DORT<sup>(22)</sup>. This was necessary to eliminate the ray effect arising from the localized nature of the external point source. The total number of neutrons emitted from the target per D-T reaction was found to be 1.0295 due to neutron multiplication in the TiT target structure. The DORT calculations were performed with  $P_3S_8$  approximations in R-Z geometry. A typical mesh size in the reflector and the test region is 0.2-0.4 cm particularly at the front surface and around measuring locations.

In treating the external neutrons by sampling from a source subroutine in the Monte Carlo calculations, the neutrons were considered to be emitted towards the whole solid angle. A typical detector size of the standard surface flux estimator is ~ 50 mm. The number of histories varied from 1-3 millions, depending on the type of response under consideration.

#### IV RESULTS AND DISCUSSION

It was previously shown that the shielded data of the multigroup analysis at deep locations in the pure SS316 assembly gives larger total neutron flux by a factor of 2 than the flux obtained with the unshielded data but this factor is only ~1.08 in the SS316/water assembly, i.e. the impact of shielding the data is less pronounced in the SS316/water assembly<sup>(10)</sup>. Similar features are observed in the current experiments.

##### A. Integrated Neutron Spectrum and High-Threshold Reaction Rates

1. Energy Rang  $E_n > 10$  MeV. The accuracy of predicting the integrated spectrum in this energy range can be judged by examining the accuracy of predicting high-threshold reactions such as the  $^{93}\text{Nb}(n,2n)^{92m}\text{Nb}$  ( $E_{th} \sim 9$  MeV) and  $^{27}\text{Al}(n,\alpha)^{24}\text{Na}$  ( $E_{th} \sim 6$  MeV). Good agreement with the experiment is observed for these reactions. Based on the FENDL/MG-1.0 data, the C/E values for the  $^{93}\text{Nb}(n,2n)^{92m}\text{Nb}$  are within ~ 2-10% of the experiment in Assembly#1 (the B<sub>4</sub>C/Pb layer installed) and ~ 5-15% in Assembly#2 (the B<sub>4</sub>C/Pb layer is not installed). The C/E values at deep locations are, however, under predicted with FENDL/MC data. The under prediction is ~ 25% in Assembly#1 and ~ 10% in Assembly#2. These features can be seen in Figs 2-3. One

can notice that the J3.1 dosimetry data gives better agreement with experiment (by ~ 2-4%).

The C/E values for the  $^{27}\text{Al}(n,\alpha)^{24}\text{Na}$  reaction are within ~ 2-10% of the experiment in Assembly#1 and within ~ 2-15% in Assembly#2 with the FENDL/MG-1.0. Again, the C/E values are under predicted at deep locations with FENDL/MC data by ~25% in Assembly#1 and by ~10-15% in Assembly#2. Identical results are obtained with J3.1 dosimetry data as compared to the results based on FENDL/MG-1.0 data. Similar to the  $^{93}\text{Nb}(n,2n)^{92m}\text{Nb}$  reaction, the results based on ENDF6/MC are larger by ~ 20% (Ass#1) and by ~10% (Ass#2) than those based on FENDL/MC at deep locations. The larger values obtained with ENDF/B-6 have been reported previously in the other experiments<sup>(6,7,10)</sup>. The features of the C/E curves for the  $^{238}\text{U}(n,f)$  reaction are similar. Generally, the effect of self-shielding is negligible for these high-threshold reactions.

The  $^{115}\text{In}(n,n')^{115m}\text{In}$  reaction is sensitive to neutrons in the energy range 1-10 MeV. The calculated values are within ~ 2-25% of experiment in Assembly#1 and within ~ 5-10% in Assembly#2 with the FENDL/MG data. The C/E values tend to be larger than unity at deep locations with FENDL/MG and the FENDL/MC, particularly in Assembly#1. The results based on FENDL/MG data are larger than those based on FENDL/MC by ~ 10-25% in Assembly#1 and by ~5-20% in Assembly#2 as can be seen from Figs. 4-5. One can notice that the over prediction is specifically observed behind the B<sub>4</sub>C/Pb layer in both assemblies and that the over prediction is lessened in Assembly#2. The features of the C/E curves in Assembly#2 are similar to the one in the SS316/water Assembly<sup>(10)</sup>. For this reaction that has a relatively low threshold energy, the self-shielding effect start to appear at deep locations.

2. Energy Rang 1 keV-1 MeV. The C/E values of the integrated spectrum in the energy range 0.1-1 MeV are shown in Fig. 6 (Assembly#1). These values are based on the MG data. Integrated spectrum is within ~ 10-25% of experiment in both Assemblies and generally over prediction is observed at deep locations. However, the prediction is within the experimental errors. In this energy range, the under prediction at deep locations in the SS316/water assembly<sup>(10)</sup> is not observed in these experiments.

The C/E values of the integrated spectrum in the energy range 1-10 keV are shown in Figs 7 (Assembly#2). These values are also obtained with the MG data. The prediction of the integrated spectrum is within ~10-20% of experiment at front locations in both assemblies. The

prediction gets worsen (~ 20-90% accuracy) in both assemblies at deep locations. The experimental errors are large at these locations (~40-90%) and therefore the predictions are within these experimental errors.

Comparison of the calculated spectrum at various locations with FENDL/MG-1.0 and FENDL/MC-1.0 data to the experimental measurement has been performed. Figures 8-9 show this comparison at depth 91.44 cm. The following can be stated on the accuracy of spectrum prediction in the energy range 1 keV-1 MeV: (1) more deviation from the experimental data occurs at deeper locations (e.g. 91.44 cm), (2) the calculated spectrum are generally larger than the measured values particularly in the energy range 10- keV to 100 keV, (3) the FENDL/MG data gives larger spectrum than those based on ENDF/MC and FENDL/MC data, (4) the MC data gives results closer to the experimental data than those obtained with the MG data, (5) the ENDF/MC data gives values larger than those obtained with the FENDL/MC data, and (6) the C/E curves have same features in both assemblies.

3. Energy range below 1 keV. The following was observed on the accuracy of the integrated neutron spectrum based on the FENDL/MG data:

3.1 Energy range 0.1-1 keV. The C/E curves are very similar in values and trends to those in found in the energy range 1-10 keV. Under prediction is observed (see Fig. 10) at mid locations ( $z=40-70$  cm) in Assembly#2 (in Assembly#1, the values are closer to unity at this depth and are within ~10% of the experiment).

3.2 Energy range 10-100 eV. The C/E curves are within ~ 2-20% of experiment in Assembly#1 and within ~ 2-25% in Assembly#2 (see Fig. 11). The trends of the curves are: (1) under prediction at front locations and over prediction at deep locations, (2) the trends are different from the SS316/water assembly (under prediction at nearly all locations, see Ref. 10). The values are generally within the experimental errors of ~ 20-25%.

3.3 Energy range 1-10 eV. The C/E values are within ~2-5% of experiment at front locations in both assemblies. There is ~10-20% under prediction at deep locations in both assemblies (see Fig. 12 for Ass.#1). Generally, there is an under prediction in the integrated spectrum at nearly all locations as in the SS316/water assembly<sup>(10)</sup>. As in the above energy ranges, the calculations are within the experimental errors (except for the deepest location).

Comparison of the calculated spectrum at various locations with FENDL/MG-1.0 and FENDL/MC-1.0 data to the experimental measurement has been performed in the energy range below 1 keV. The general observations on the accuracy of the calculations are as follows:

#### 3.4 Shallow locations in both assemblies. (1)

Good agreement with the experimental data within the experimental errors and within the Monte Carlo statistics at almost all shallow locations up to a depth 45.7 cm with all data bases. (2) The shielded data of FENDL/MG gives results with better agreement with the experiment than the results based on the unshielded data. (3) The continuous Monte Carlo data gives results with better agreement with the measured data than those based on the MG data. Figure 13 gives spectrum comparison at depth 127mm in Assembly#1.

#### 3.5 Deep locations in both assemblies. (1)

The largest deviation from the experimental data occurs at location 71.12 cm where all calculated spectra fall below the experimental data. This could be attributed to the accuracy in specifying the exact location and/or the accuracy in specifying the atomic densities of materials at this location. (2) At other locations, the FENDL/MG data gives larger spectrum than measurements above 50 eV and lower values than measurements below this energy. (3) At these deep locations, the Monte Carlo data gives larger spectrum than the results based on the MG data, particularly at energies below 50 eV. Figure 14 gives spectrum comparison at depth 914.4 mm in Assembly#1.

### B. Non-Threshold Reaction Rates

The C/E values of the  $^{197}\text{Au}(n, \gamma)^{198}\text{Au}$  reaction are shown in Figs. 15-16 in Ass.#1. In both assemblies, there is an under prediction at nearly all locations and the calculated values are not within the experimental errors. With the FENDL/MG data and at front locations, the C/E values are below unity by ~ 5-10% in Assembly#1 and by ~2-20% in Assembly#2. At deep locations, the C/E values fall below unity by ~60-80% in both Assemblies. The under estimation at deep locations are similar in feature to the one found in the SS316/water experiment<sup>(10)</sup> but this under estimation is larger in these SCM experiments. One notices also that the C/E values improve upon using J3.1 dosimetry cross-section. The under prediction could be attributed to the under prediction in the integrated spectrum below 1 eV (as is the case with  $^{10}\text{B}(n, \alpha)^7\text{Li}$  reaction which has similar C/E curves, see Figs. 17-18). The effect of self-shielding is clear in this case, particularly at deep locations. Shielded data give better agreement with the experiment. With the Monte Carlo data, the under prediction is much lessened compared to those based on the MG data. This is because the Monte Carlo data gives larger spectra at very low energies than the spectra obtained with the MG data (see Fig. 14). Much improvement (by at least 30%) occurs with the shielded FENDL/MG data. This is more apparent in the  $^{10}\text{B}(n, \alpha)^7\text{Li}$  reaction.

The C/E values of the  $^{235}\text{U}(n,f)$  reaction are shown in Figs. 19-20. With the MG data, the C/E values are within ~ 5-30% of experiment in both assemblies. As is the case for the other non-threshold reactions, the calculations are not within the experimental errors. The C/E curves are similar in both assemblies. The trend is under estimation at front locations and slight over estimation at deep locations. The largest discrepancy occurs at depth ~70 cm. The effect of self-shielding is apparent for this non-threshold reaction. Again, the results based on the FENDL/MC data are closer to the experimental values. The MC results are larger than those obtained with the MG data for the same reason discussed above.

### C. Gamma-Rays Spectrum

The gamma-ray spectra at several locations were calculated with the FENDL/MG data base. The calculated spectrum reproduce the experimental data fairly well, except at energies above 10 MeV. The experimental errors at this high-energy range are generally large as can be seen from Fig. 21.

### D. Gamma-Ray Nuclear Heating

The gamma-ray kerma factors for SS316, epoxy glass and copper were folded with the gamma-ray spectrum to calculate gamma-ray heating at each location. The C/E values of gamma-ray heating in SS316, epoxy, and copper are shown in Figs. 22, 23, and 24, respectively. The results shown in these figures are based on the FENDL/MG data. As for the SS316 case, C/E values are within ~5-10% of the experiment in both assemblies at front locations. The C/E values are larger than unity by ~25% in Assembly#1 and by ~30% in Assembly#2 at the back locations. The C/E values in the epoxy are below unity by ~ 5-20% at front locations in both assemblies but larger than unity by ~ 10% in Assembly#1 and by ~ 25% in assembly#2. There is an under estimation in the heating rate in the copper at front locations by ~ 2-20% in Assembly#1 but the values are within 10% in Assembly#2. Like the SS316 and epoxy cases, the heating rate is over estimated by ~ 10 in Assembly#1 and by ~ 25% in Assembly#2 at deep locations. Notice however that the experimental errors are large (~20%) at these deep locations.

## V CONCLUDING SUMMARY

The prediction accuracy of several neutronics parameters has been examined in integral experiments performed on a large SS316/water bulk shield assembly that includes a zone simulating the super conducting magnet placed at the back of the ITER shield blanket. These experiments were conducted to resolve some of the R&D issues pertaining to the nuclear design of ITER

blanket, among which is the accuracy of the newly developed data base, FENDL-1. Both deterministic and Monte Carlo analyses were undertaken to arrive at estimate to the uncertainty involved in calculating these parameters with various codes and data bases. Among the parameters measured and compared to prediction: (a) neutron spectrum below 2 MeV, (b) foil activation rates such as Nb-93(n,2n)Nb-93m, Al-27(n, $\alpha$ )Na-24, In-115(n,n')In-115m, Au-197(n, $\gamma$ )Au-198, and B-10(n, $\alpha$ )Li-7, (c) fission rate U-235(n,f) and U-238(n,f), (d) gamma-ray spectrum, and (e) gamma-ray heating rate. More details of the results cited in this paper can be found in Ref. 23.

The high-threshold reaction Nb-93(n,2n) is sensitive to the integrated spectrum above 10 MeV and is well predicted within 2-15% of the experiments with an over-prediction, a trend that is reverse to what was found in previous experiments on SS316/water experiment. Similar accuracy (2-10% in Assembly#1 and 2-15% in Assembly#2) were obtained for the Al-27(n, $\alpha$ ) and U-238(n,f) reactions. The calculated-to-experiment (C/E) values for the In-115(n,n') reaction are within 2-25% of the experiment, where over-prediction is observed behind the B,C/Pb layer in Assembly#1. One can generally state that these high-threshold reactions are predicted with an uncertainty that does not exceed 25%.

The integrated spectrum in the range 0.1-1 MeV is within 10-25% in both assemblies and generally an over prediction is observed at deep location, a reverse trend to what was found in the SS316/water experiment. Large discrepancy was found in the integrated spectrum in the range 1-10 keV (C/E ~1.9) at deep locations but the experimental errors are large (20-90%) at these locations. It is observed that in the energy range 1 keV-1MeV, the FENDL/MG data gives larger spectrum than those based on ENDF/MC and FENDL/MC data. Below 1 keV and at deep locations, the FENDL/MG data gives larger spectrum than measurements above 50 eV and lower values below this energy. At these locations, the Monte Carlo data gives larger spectrum than the MG data, particularly at energies below 50 eV. This is reflected on the low energy (non-threshold) reaction rates which are sensitive to neutrons in the energy range below 1 eV [e.g. Au-197(n, $\gamma$ ), B-10(n, $\alpha$ ), U-235(n,fission)] where the C/E values based on the MC data are larger than those obtained with the MG data. Generally, the MC data gives results closer to the experimental data. It is suspected that the integrated spectrum is under predicted below 1 eV as inferred by the B-10(n, $\alpha$ ) reaction which is under predicted by 15-60% and by the  $^{197}\text{Au}(n,\gamma)^{198}\text{Au}$  reaction which is under predicted by ~ 60-80% at deep locations. This under prediction is more apparent with the MG data. This could

be caused by the inaccuracy in the thermal group cross-sections used in the multi-group FENDL library

Gamma-ray flux is well reproduced within the experimental error, except at energies above 10 MeV where large discrepancies are observed. The gamma-ray heating rates in SS316, epoxy glass, and copper are well predicted at front locations (within the experimental errors of ~ 20%). However, there is an over estimation of ~20-25% at deep locations.

ACKNOWLEDGMENT

This work is supported by the U.S. Department of Energy grant#DOE-FG03-88ER52150.. This paper is partly an account of work assigned to the U.S. Home Team under ITER Task Agreement T218: "Shielding Neutronics Experiment" within the Agreement among the European Atomic Energy Community, the Government of Japan, the Government of the Russian Federation, and the Government of the United States of America on Cooperation in the Engineering Design Activities for the International Thermonuclear Experimental Reactor ("ITER EDA Agreement") under the auspices of the International Atomic Agency (IAEA).

Table 1 Atomic Densities of Materials Used in the Analysis

Nuclide**	SS316 (Test Region)	SS316 (Reflector Region)	Air	Water
H-1 (E/B6.1) N-14 (B2) O-16 (E/B6.0)			3.8810e-5 1.0400e-3	6.6659e-2 3.3329e-2
Si (B2) Cr (E/B6.1) Mn-55 (E/B6.1) Fe (E/B6.1) Ni (E/B6.1)* Mo (J3.1)	1.0341e-3* 1.5482e-2 1.0355e-3 5.7904e-2 9.3410e-3 1.0590e-3	8.1608e-4 1.5025e-2 1.3560e-3 5.8331e-2 9.1460e-3 1.0250e-3	- - - - -	- - - - -
Nuclide**	SS316 (In SCM)	B4C	Epoxy Glass	SCM
H-1 (E/B6.1) O-16 (E/B6.0)			9.3210e-3 2.4184e-2	5.7360e-3 5.1340e-3
B-10 (E/B6.1) B-11 (E/B6.0) C (E/B6.1) Mg (J3.1) Al (J3.1) Ca (J3.1) Ti (J3.1) Cu (E/B6.2) Nb (B2) Ta (J3.1) Br Si (B2) Cr (E/B6.1) Mn-55 (E/B6.0-J3) Fe (E/B6.1) Ni (E/B6.1)* Mo (J3.1)		2.0148e-2 8.7519e-2 2.6924e-2	4.6900e-4 1.7070e-3 1.3372e-2 5.3000e-4 2.0420e-3 2.6320e-3 2.9490e-3 6.5120e-3	9.0000e-3 3.2300e-4 5.2390e-3 1.0200e-4 3.8800e-4 5.0200e-4 4.3900e-3 3.0016e-2 3.4870e-3 6.4500e-4 1.2390e-3

\* Reads: 1.0341 X 10<sup>3</sup> X 10<sup>24</sup> atoms/cm<sup>3</sup> Atomic Density of Pb: 3.2523e-2  
 \*\* E/B6.1 (ENDF/B-V1.1); B2: BROND-2  
 J3.1: JENDL-3.1 + Except Ni-61 (from E/B6.0)

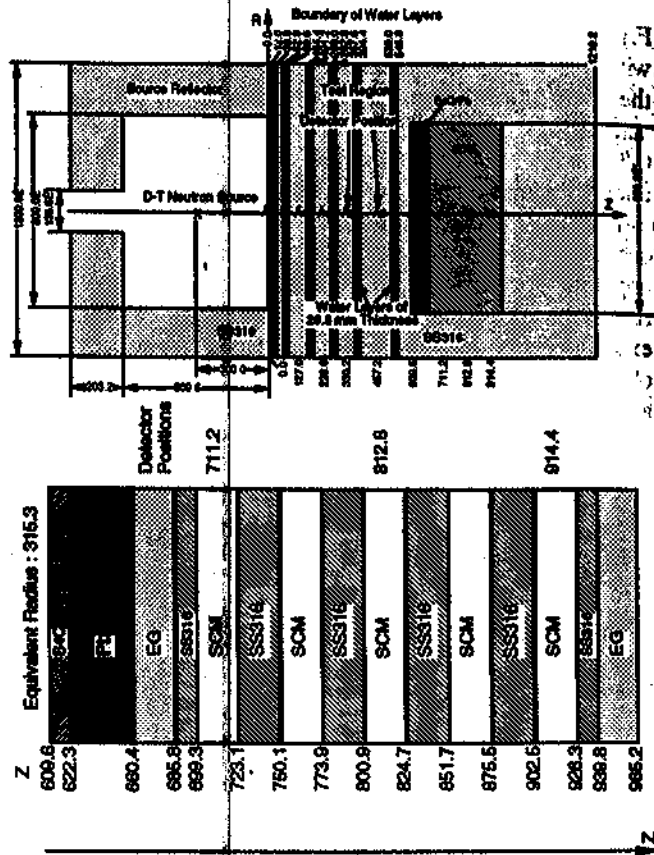


Figure 1: The Geometrical (R-Z) Model of the SS316/Water Assembly With a Simulated Super Conducting Magnet

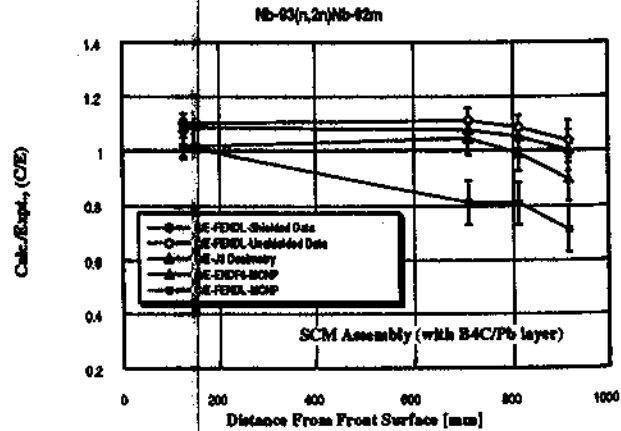


Figure 2: C/E Values for the Nb-93(n,2n)Nb-93m Reaction -SCM Assembly with B,C/Pb layer

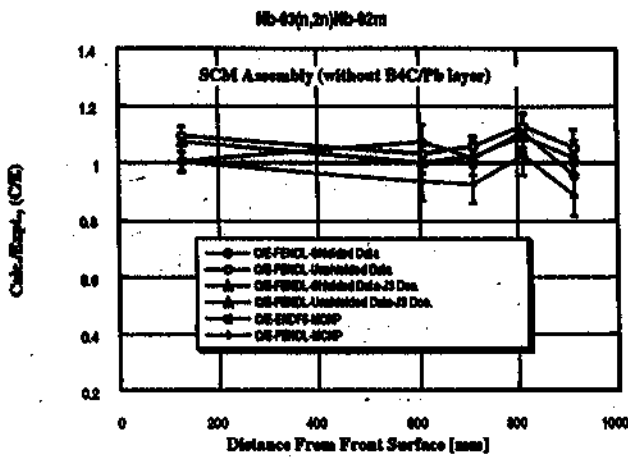


Figure 3: C/E Values for the Nb-93(n,2n)Nb-93m Reaction -SCM Assembly without B,C/Pb layer

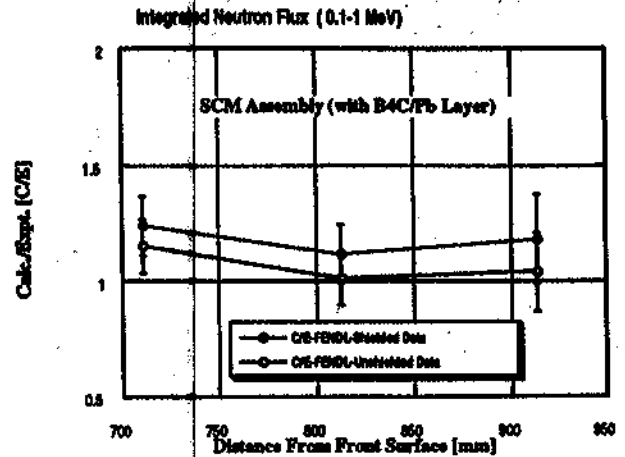


Figure 6: C/E Values of the Integrated Neutron Spectrum in the Range 0.1- 1 MeV - SCM Assembly with B,C/Pb

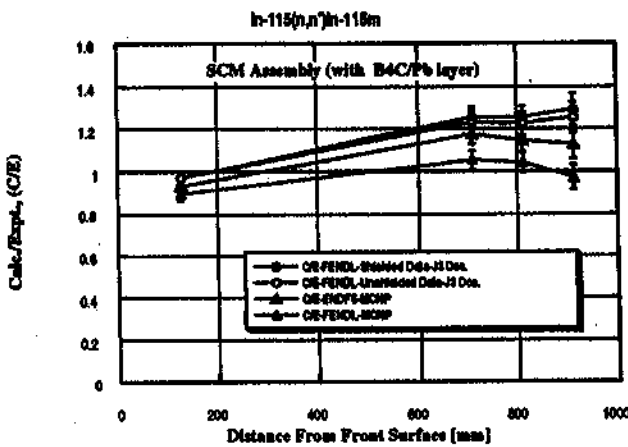


Figure 4: C/E Values for the In-115(n,n')In115m Reaction - SCM Assembly with B,C/Pb layer

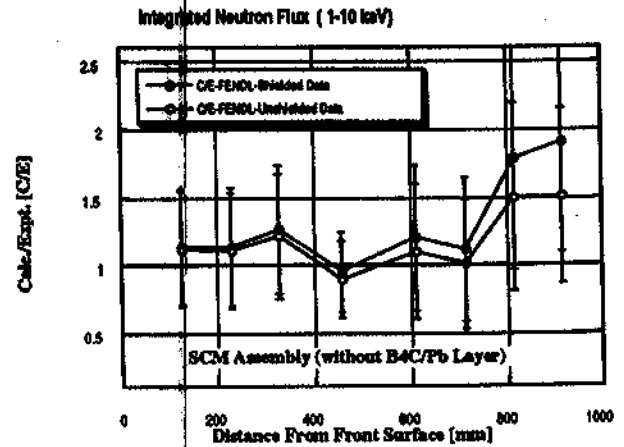


Figure 7: C/E Values of the Integrated Neutron Spectrum in the Range 1 - 10 keV - SCM Assembly without B,C/Pb

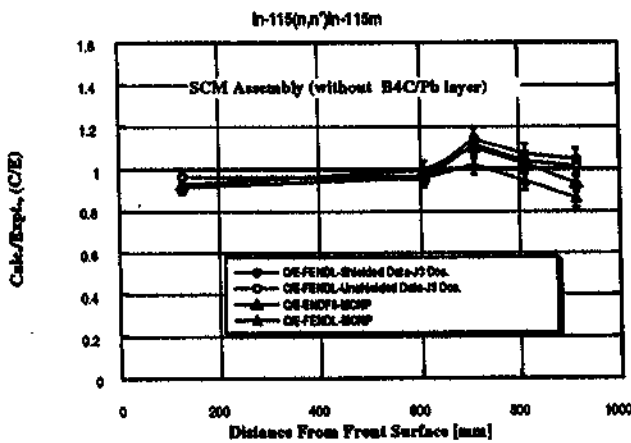


Figure 5: C/E Values for the In-115(n,n')In115m Reaction - SCM Assembly without B,C/Pb layer

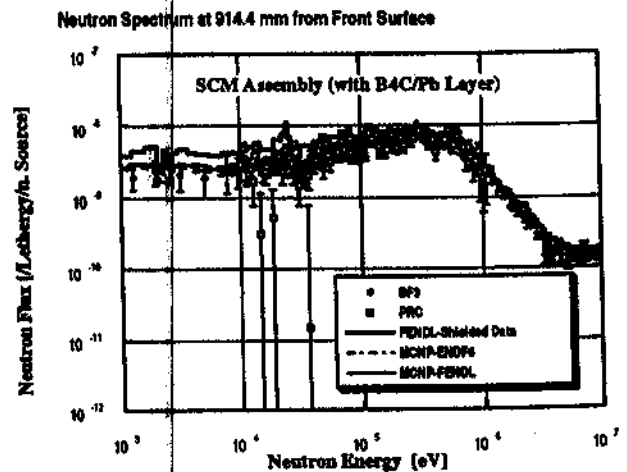


Figure 8: Neutron Spectrum at 914.4 mm from Front Surface in the keV Energy Range-SCM Assembly with B,C/Pb Layer.



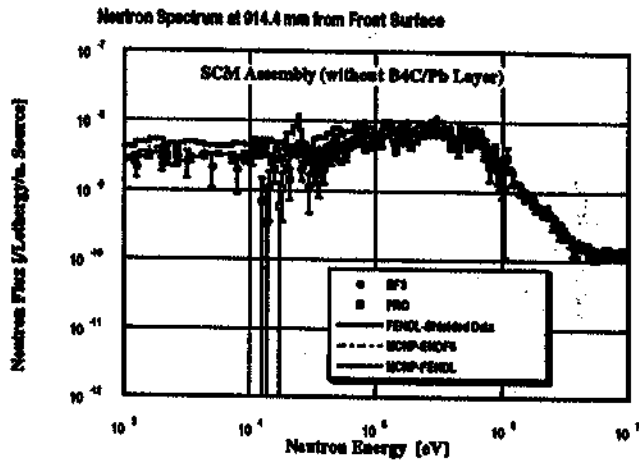


Figure 9: Neutron Spectrum at 914.4 mm from Front Surface in the keV Energy Range-SCM Assembly without B,C/Pb Layer.

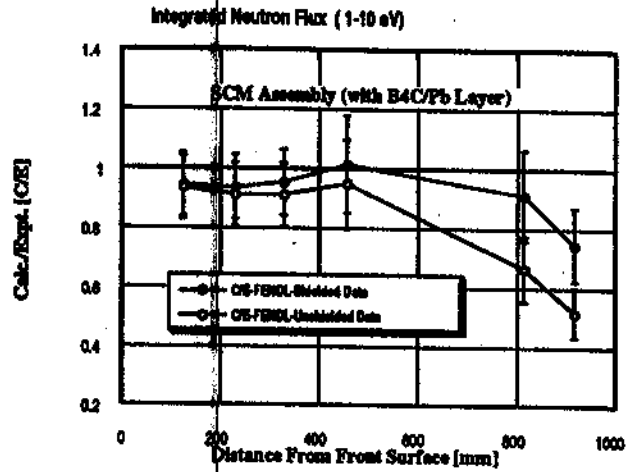


Figure 12: C/E Values of the Integrated Neutron Spectrum in the Range 1-10 eV-SCM Assembly with B,C/Pb layer.

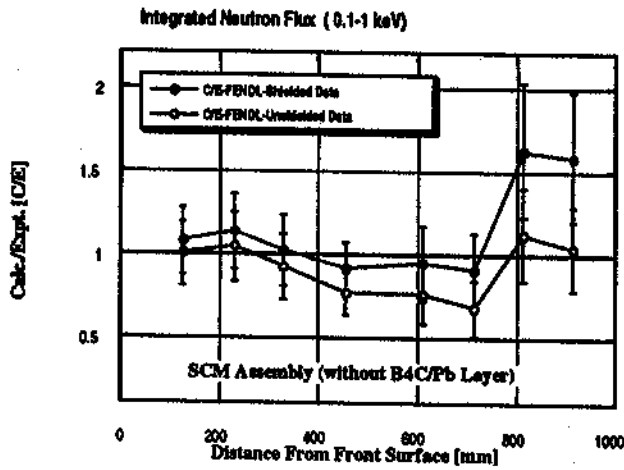


Figure 10: C/E Values of the Integrated Neutron Spectrum in the Range 0.1 - 1 keV-SCM Assembly without B,C/Pb

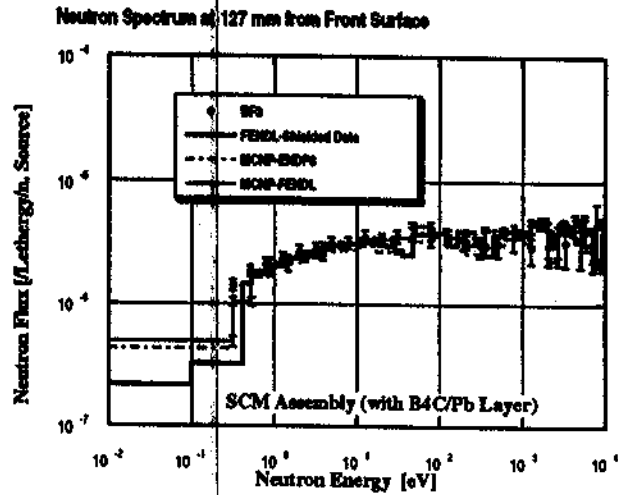


Figure 13: Neutron Spectrum at 127 mm from Front Surface - eV Energy Range-SCM Assembly with B,C/Pb

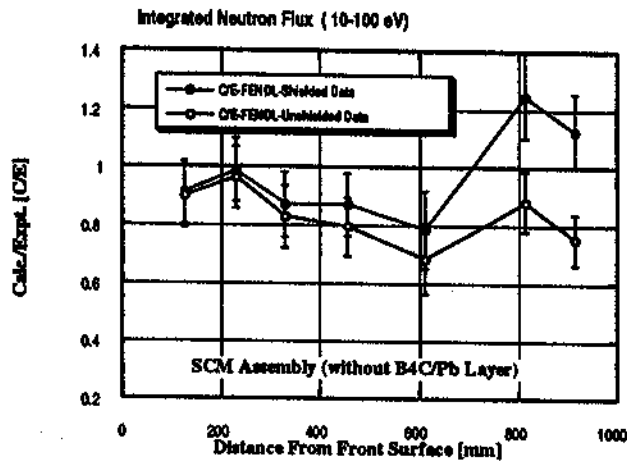


Figure 11: C/E Values of the Integrated Neutron Spectrum in the Range 10-100 eV-SCM Assembly without B,C/Pb

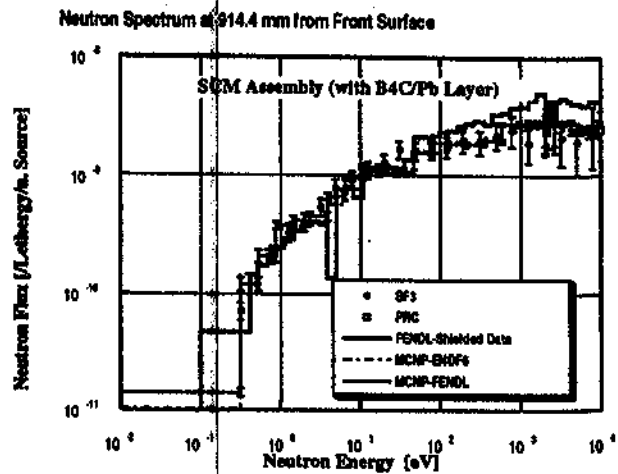


Figure 14: Neutron Spectrum at 914.4 mm from Front Surface - eV Energy Range-SCM Assembly with B,C/Pb



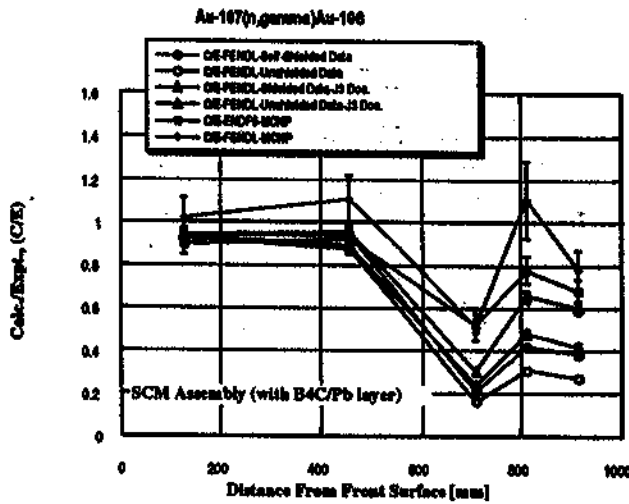


Figure 15: C/E Values for the Au-197(n,gamma)Au-198 Reaction -SCM Assembly with B,C/Pb layer.

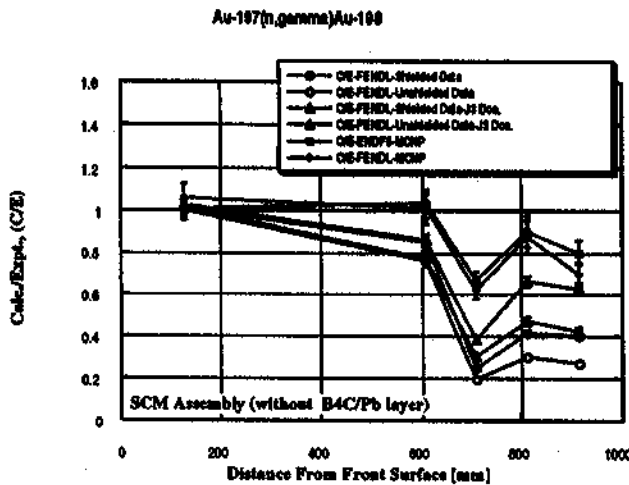


Figure 16: C/E Values for the Au-197(n,gamma)Au-198 Reaction -SCM Assembly without B,C/Pb layer.

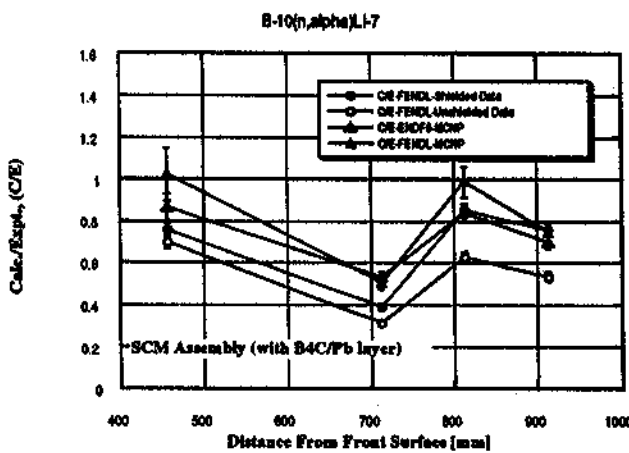


Figure 17: C/E Values for the B-10(n,alpha)Li-7 Reaction -SCM Assembly with B,C/Pb layer.

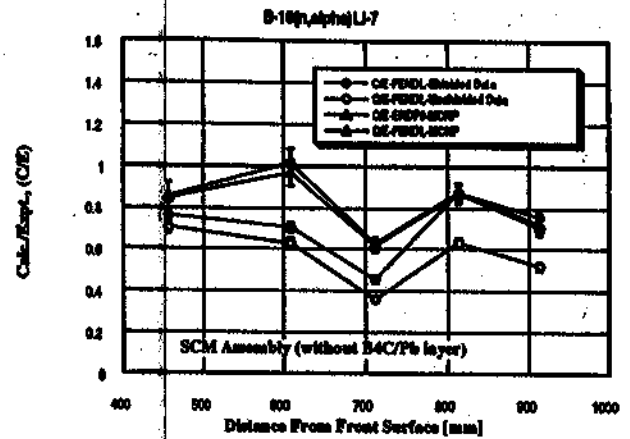


Figure 18: C/E Values for the B-10(n,alpha)Li-7 Reaction -SCM Assembly without B,C/Pb layer.

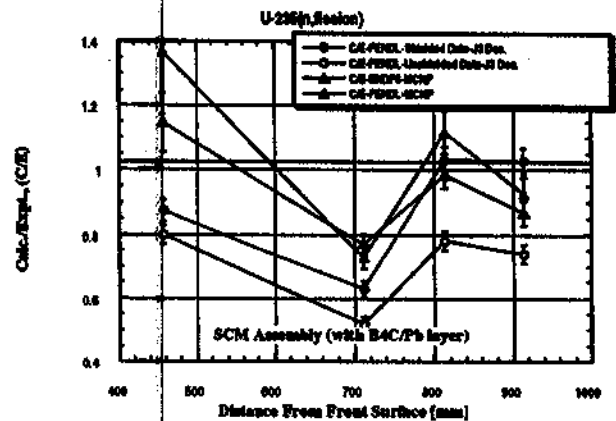


Figure 19: C/E Values for the U-235(n,fission) Reaction -SCM Assembly with B,C/Pb layer.

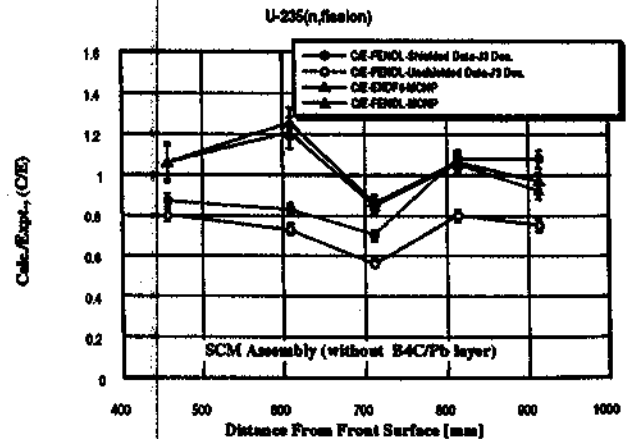


Figure 20: C/E Values for the U-235(n,fission) Reaction -SCM Assembly without B,C/Pb layer.

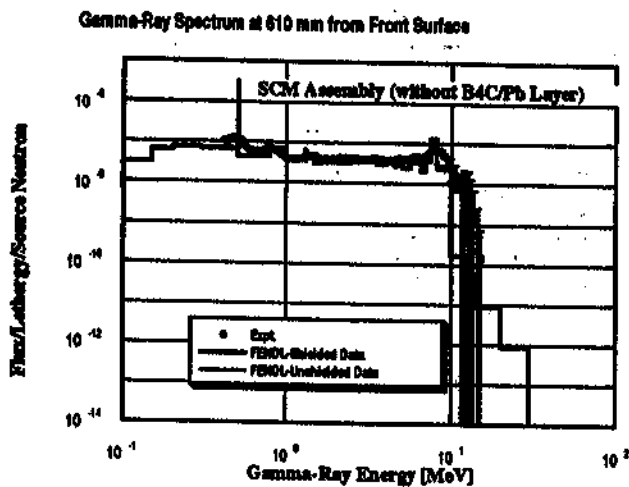


Figure 21: Gamma-ray Spectrum at 610 mm From Front Surface-SCM Assembly Without B,C/Pb Layer.

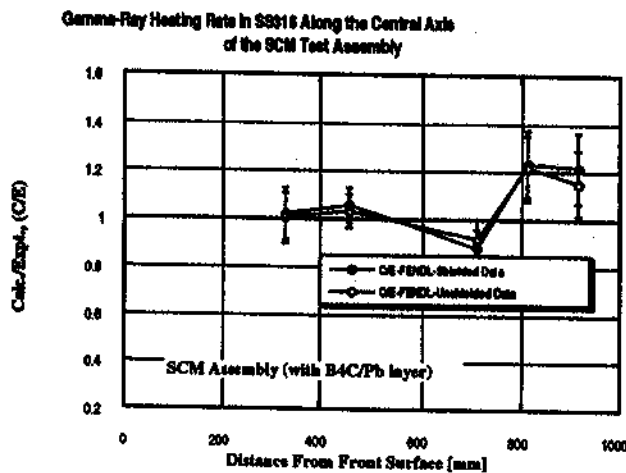


Figure 22: C/E Values of Gamma-ray Heating Rate in SS316 Along the Central Axis-SCM Assembly with B,C/Pb Layer.

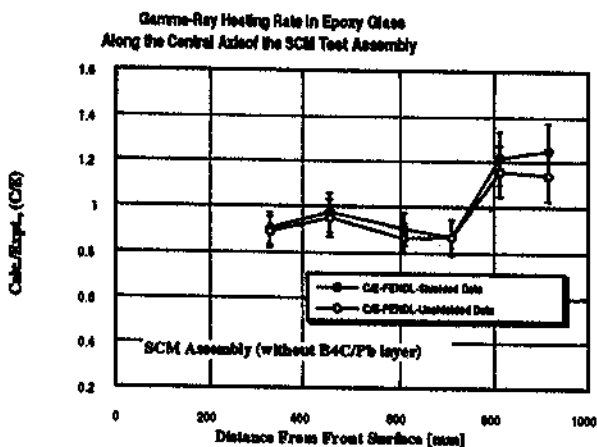


Figure 23: C/E Values of Gamma-ray Heating Rate in Epoxy Along the Central Axis-SCM Assembly without B,C/Pb Layer.

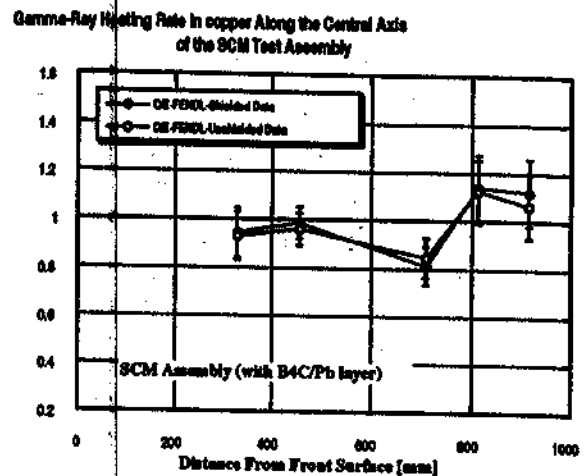


Figure 24: C/E Values of Gamma-ray Heating Rate in Copper Along the Central Axis-SCM Assembly with B,C/Pb Layer.

REFERENCES

1. "ITER Conceptual Design Report," ITER Documentation Series, No 18, IAEA, Vienna (1991)
2. Glass, A.J., "Status and Plans for ITER," J. of Fusion Energy, Vol. 11, No. 2, 1992
3. "Technical Basis for ITER Detail Design Report, Cost, Review, and Safety Analysis", ITER Document, International Thermonuclear Experimental Reactor, (November 1996)
4. C. Konno, F. Maekawa, Y. Oyama, Y. Ikeda, K. Kosako, And H. Maekawa, "Bulk Shielding Experiments on Large SS316 Assemblies Bombarded By D-T Neutrons, Volume I: Experiment", JAERI-Research-94-043, Japan Atomic Energy Research Institute, (December, 1994)
5. F. Maekawa, C. Konno, K. Kosako, Y. Oyama, Y. Ikeda, And H. Maekawa, "Bulk Shielding Experiments on Large SS316 Assemblies Bombarded By D-T Neutrons, Volume II: Analysis", JAERI-Research-94-044, Japan Atomic Energy Research Institute, (December, 1994)
6. M.Z. Youssef, et al., "Benchmarking FENDL-1.0 Library Through Analysis Of Existing Experiments, Part (I): Analysis Of Bulk Shielding Experiments On Large SS316 Assemblies Bombarded By D-T Neutrons, ITER/US/95/VI-BL-14A, UCLA-FNT-90, UCLA-ENG-94-40, University of California, Los Angeles, (December, 1994)

7. M.Z. Youssef, A. Kumar, M.A. Abdou, C. Konno, F. Maekawa, M. Wada, Y. Oyama, H. Maekawa, and Y. Ikeda, "Benchmarking FENDL Libraries Through the Analysis of Bulk Shielding Experiments on Large SS316 Assemblies for the Verification of ITER Shielding Characteristics, Fusion Technology, Vol. 30, 1101-1112 (December 1996)
8. C. Konno, et al., "Bulk Shielding Experiments on Large SS316/Water Assemblies Bombarded By D-T Neutrons, Volume I: Experiment," JAERI-Research 95-017, Japan Atomic Energy Research Institute, (March 1995)
9. F. Maekawa, et al., "Bulk Shielding Experiments on Large SS316/Water Assemblies Bombarded By D-T Neutrons, Volume II: Analysis, JAERI-Research 95-018, Japan Atomic Energy Research Institute, (March 1995)
10. M.Z. Youssef, A. Kumar, M. Abdou, C. Konno, F. Maekawa, M. Wada, Y. Oyama, H. Maekawa, and Y. Ikeda, "Verification of ITER Shielding Capability and FENDL Data Benchmarking Through Analysis of Bulk Shielding Experiment on Large SS316/Water assembly Bombarded With 14 MeV Neutrons", Proc. of International Symposium on Fusion Nuclear Technology, ISFNT-4, April 6-11, 1997, Tokyo, Japan, Will appear as special issue, Fusion Engineering and Design, (1998)
11. S. Ganesan, and D.W. Muir, "FENDL Multigroup Libraries," IAEA-NDS-129, International Atomic Energy Agency, (July 1992)
12. S. Ganesan, "Improved Evaluations and Integral Data Testing for FENDL: Summary Report of the IAEA Advisory Group Meeting organized by the International Atomic Energy Agency in co-operation with MAX-Planck Institute fur Plasmaphysik, Garching near Munich, Germany, 12-16 December, 1994, INDC(NDS)-312, International Nuclear Data Committee, IAEA, November, 1994
13. A.B. Pashchenko, Completion of FENDL-1 and Start of FENDL-2, INDC(NDS)-352, IAEA Nuclear Data Section, International Atomic Energy Agency, (March 1996)
14. A.B. Pashchenko, "The IAEA Advisory Group Meeting on Extension and Improvement of the FENDL Library for Fusion Applications (FENDL-2)", minutes of the meeting held March 3-7, 1997, Vienna, Austria, to be published (1997)
15. U. Fischer, Editor, "Integral Data Tests of the FENDL-1 Nuclear Data Library for Fusion Application, Summary Report of the International Working Group, Experimental and Computational Benchmarks on Fusion Neutronics Validation", FZKA 5785, INDC (GER)-41, Forschungszentrum Karlsruhe, (August 1996)
16. P. Batistoni, et al., "2nd Intermediate Report on Measurements and Analysis: ITER Task 218 on Shielding Neutronics Experiment, Subtask A/ EU Contribution", prot. n.11/97 TECN/NEU, ENEA C.R., Frascati, Italy, (January 1997)
17. M. Nakagawa and T. Mori, "MORSE--DD, A Monte Carol Code Using Multigroup Double Differential Form Cross-Sections" JAERI-M84-126, Japan Atomic Energy Research Institute, July, 1984.
18. M. Nakazawa, et al., "JENDL Dosimetry File," JAERI-1325 (1992)
19. R.E. MacFarlane, "TRANSX2: A Code for Interfacing MATXS Cross-Section Libraries to Nuclear Transport Codes," LA-12312-MS, UC-705 and UC-700 Issued: July 1992, Los Alamos National Laboratory, (1992)
20. R.E. MacFarlane, Los Alamos National Laboratory, private communications, 1994
21. L.P. Ku and J. Kolibal. "RUFF-A Ray Tracing Program to Generate Uncollided Flux and First Collision Source Moments for DOT4. A User's Manual. EAD-R-16, Plasma Physics Laboratory, Princeton University, (1980).
22. Rhoades, W.A., and Childs, R.L., "The DORT: Two-Dimensional Discrete Ordinates Transport Code", Nuc. Sci. & Engrg., 99, pp. 88-89 (May 1988), Also, see CCC-484, Radiation Shielding Information Center (1988).
23. M.Z. Youssef, A. Kumar, and M.A. Abdou, "Analysis Of Simulated Super Conducting Magnet Experiments On Large SS316/Water Assembly Bombarded With 14 MeV", UCLA-FNT-101, UCLA-ENG-98-191, University of California, Los Angeles, (April, 1998)